

# A new approach for quantitative damage assessment of in-situ rock mass by acoustic emission

Jin-Seop Kim<sup>1a</sup>, Geon-Young Kim<sup>1a</sup>, Min-Hoon Baik<sup>1a</sup>, Stefan Finsterle<sup>2b</sup> and Gye-Chun Cho<sup>\*3</sup>

<sup>1</sup>Radioactive Waste Technology Development Division, Korea Atomic Energy Research Institute, Daejeon 305-353, Korea

<sup>2</sup>Finsterle GeoConsulting, Kensington, CA 94708, U.S.A.

<sup>3</sup>Department of Civil & Environmental Engineering, Korean Advanced Institute for Science and Technology, Daejeon 305-701, Korea

(Received April 6, 2018, Revised April 7, 2019, Accepted April 8, 2019)

**Abstract.** The purpose of this study was to propose a new approach for quantifying in situ rock mass damage, which would include a degree-of-damage and the degraded strength of a rock mass, along with its prediction based on real-time Acoustic Emission (AE) observations. The basic approach for quantifying in-situ rock mass damage is to derive the normalized value of measured AE energy with the maximum AE energy, called the degree-of-damage in this study. With regard to estimation of the AE energy, an AE crack source location algorithm of the Wigner-Ville Distribution combined with Biot's wave dispersion model, was applied for more reliable AE crack source localization in a rock mass. In situ AE wave attenuation was also taken into account for AE energy correction in accordance with the propagation distance of an AE wave. To infer the maximum AE energy, fractal theory was used for scale-independent AE energy estimation. In addition, the Weibull model was also applied to determine statistically the AE crack size under a jointed rock mass. Subsequently, the proposed methodology was calibrated using an in situ test carried out in the Underground Research Tunnel at the Korea Atomic Energy Research Institute. This was done under a condition of controlled incremental cyclic loading, which had been performed as part of a preceding study. It was found that the inferred degree-of-damage agreed quite well with the results from the in situ test. The methodology proposed in this study can be regarded as a reasonable approach for quantifying rock mass damage.

**Keywords:** acoustic emission; quantitative damage; rock mass; wave attenuation; fractal theory; Wigner-Ville distribution; Weibull model

## 1. Introduction

After the installation of high-level nuclear waste including spent fuel into a nuclear waste repository, generally more than 100 years of dynamic monitoring and facility operation are to be followed before closure of the system for permanent disposal. Recently, there has been a tendency to adopt a delayed approach (phasing) as part of the waste disposal management options (EC 2004a). The retrievability, long-term underground storage, and interim storage are under discussion as radioactive waste management options, all of which are highly influenced by social, political or economic concerns. Even if an alternative management option is adopted rather than the geological disposal concept, the introduction of such a new option will also result in increased requirements for the geomechanical stability of open spaces and the safety issues in a radioactive repository. Thus, the long-term stability and durability of a disposal system cannot be ignored regardless of which disposal management option is selected in the future. Therefore, the real-time monitoring of repository

integrity and subsequent damage analysis is a very important issue from the perspective not only of the long-term performance assessment of a repository, but also a matter of confidence building in the peripheral society.

Because Acoustic Emissions (AE) are highly sensitive to the initiation and growth of cracks in materials, they have long been recognized as an efficient method for real-time monitoring of structural health, and widely used to evaluate various types of damage such as fatigue, dislocation, corrosion, and crack growth in a variety of geotechnical underground structures and nuclear facilities (Hardy 1994, ASTM 1981, Wang *et al.* 2009). In a nuclear waste repository, the AE technique has also been used for real-time microseismic observations. Atomic Energy of Canada Limited (AECL) performed a Mine-by Experiment at the Underground Research Laboratory (URL) for monitoring rock mass behaviors and damage development using an acoustic emission/microseismic (AE/MS) monitoring system (Martin and Read 1996). The Swedish Nuclear Fuel and Waste Management Co. (SKB) used microseismic monitoring to quantify rock fracturing in the Zedex Experiment (Emsley 1997). Cai *et al.* (2001) studied a method to characterize rock mass damage based on microseismic monitoring and presented a damage-driven numerical model for rock mass behavior simulation. Tang *et al.* (2015) and MA *et al.* (2017) analyzed the stability of highly steep rock slope by microseismic AE monitoring. Eberhardt *et al.* (1998) and Martin and Chandler (1994)

\*Corresponding author, Professor

E-mail: [gyechun@kaist.edu](mailto:gyechun@kaist.edu)

<sup>a</sup>Ph.D., Principal Researcher

<sup>b</sup>Ph.D., Executive Manager

tried to correlate cumulative AE counts with an observed decrease in the elastic stiffness and cohesive strength of the material under consideration. Rao and Ramana (1992) investigated the progressive failure of rock under cyclic loading based on the measurement of ultrasonic wave velocities and AE events. Meng *et al.* (2018) evaluated AE characteristics of red sandstone under conditions of uniaxial cyclic loading and unloading of compression. Yang *et al.* (2013) carried out triaxial compression experiments to investigate strength and deformation failure behavior of rock using an AE technique under simple and complex loading. Kim *et al.* (2014) and Jin *et al.* (2017) indicated that the damage parameters derived from a mechanically measured inelastic volumetric strain (plastic strain) were closely related to those from physically detected AE waves. Although the AE technique has been regarded as a promising method for real-time monitoring of a waste repository (EC 2004b, IAEA 2001), very few studies have been made using AE monitoring to quantify rock mass damage in situ.

The objective of this study was, therefore, to propose a new approach for quantifying in situ rock mass damage, that is, to provide a degree-of-damage estimate and the corresponding degraded strength of the rock mass, and to predict this damage based on real-time AE observations. Subsequently, the proposed methodology was calibrated by comparing the inferred degree-of-damage with that from an in situ test that had been previously performed in the Underground Research Tunnel (KURT) at the Korea Atomic Energy Research Institute (KAERI). The methodology was developed based on the various theoretical approaches to overcome the effects from in situ conditions on the AE characteristics. These approaches included the time-frequency algorithm of Wigner-Ville Distribution (WVD) (Wigner 1932, Ville 1948) with Biot's wave dispersion model for a more reliable AE source location, the statistical Weibull model (Weibull 1951) for crack size determination, in situ wave attenuation for AE energy correction in the rock mass, and finally, a fractal theory for scale-independent AE energy. The detailed procedures for utilization of the proposed methodology for quantifying the rock mass damage are provided at the end of this paper.

## 2. Review of previous in-situ studies

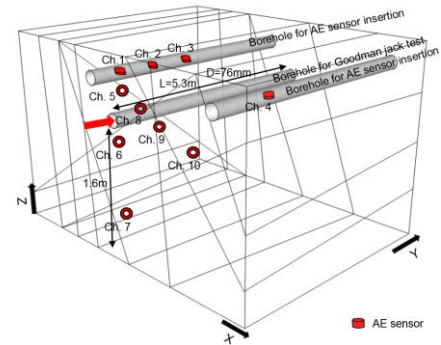
As part of the research preceding this paper, Kim (2013) obtained a damage evolution curve (normalized degree of damage versus normalized stress) of a rock mass under a dynamic loading condition from in-situ tests, in which a Goodman Jack test and simultaneous AE monitoring were carried out in the KURT (Fig. 1). The plat of Goodman Jack was loaded radially in a bi-axial direction in the borehole (indicated by a red arrow in Fig. 1(b)). The detailed experimental procedures, apparatus and data analysis method are available in the literature (Kim 2013).

$$\frac{E_{AE}}{E_{max.AE}} = a \left( \frac{\sigma}{\sigma_c} \right)^b \exp \left\{ c \left( \frac{\sigma}{\sigma_c} \right) \right\} \quad (1)$$

where  $E_{AE}$  is the cumulative AE energy,  $E_{max.AE}$  is the maximum cumulative AE energy at failure,  $E_{AE}/E_{max.AE}$

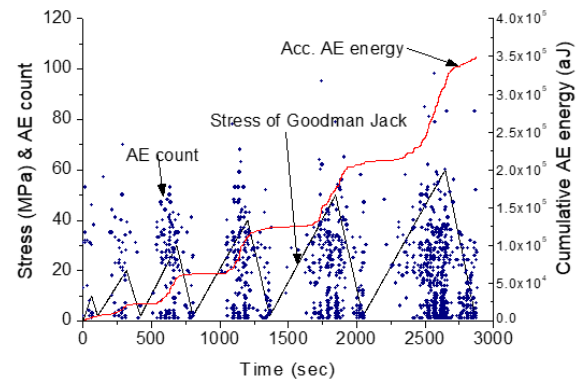


(a)

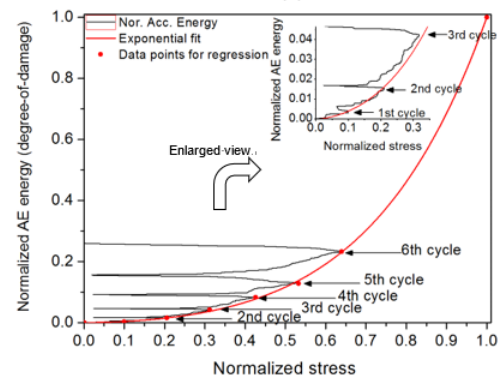


(b)

Fig. 1 Experimental setup at KURT: (a) Goodman Jack and DAQ system and (b) AE sensor locations



(a)



(b)

Fig. 2 Primary results from the previous study: (a) variation in stress and AE energy over time from the Goodman Jack test, and (b) in situ damage evolution curve of KURT rock mass (the dots in the graph are the points used for the derivation of the regression curve) (Kim 2013)

indicates the damage parameter  $D$ ,  $\sigma$  is the stress,  $\sigma_c$  is the peak strength of the rock mass, and  $a$ ,  $b$ , and  $c$  are the experimental constants.

The variations in stress and detected AE counts over time during the in situ test, are shown in Fig. 2(a). Normalized AE energy means the damage to the rock mass (Kim *et al.* 2014). The solid line in Fig. 2(b) stands for the damage evolution curve, and was formulated as Eq. (2) based on the general shape of Eq. (1).

$$\frac{E_{AE}}{E_{maxAE}} = 0.119 \left( \frac{\sigma}{\sigma_c} \right)^{1.562} \exp(2.132 \frac{\sigma}{\sigma_c}) \quad R^2 = 0.998 \quad (2)$$

### 3. Proposed methodology for damage quantification

All the in situ data used for the methodology development were derived from Kim (2013). A flow scheme of this study is presented in Fig. 3. The basic approach was first to identify where the AE cracks were generated in the rock mass and to determine the AE crack size in rock mass. Subsequently, it was necessary to infer the maximum AE energy, which is used for normalizing the AE energy measured in situ. The value of the measured AE energy normalized using the maximum AE energy is the degree-of-damage. With regard to estimation of the maximum AE energy, a fractal theory was applied to provide scale-independent maximum AE energy, in which the in situ attenuation of AE waves was also taken into account during the process of data analysis.

#### 3.1 AE crack size determination

##### 3.1.1 AE source location in a jointed rock mass

The degree-of-damage of a rock mass greatly depends on how reliable the AE source location is. The source location of the AE event was first determined using a combined method of WVD with a theoretical wave dispersion model, which was recently proposed by Kim *et al.* (2013). This algorithm is known to be applicable to the AE source location in jointed rock mass.

Only the data detected simultaneously by all the AE sensors were selected for the analysis. A total of 182 data were used to provide 3D AE source localization. The representative time-frequency analyses using WVD and the theoretical wave model are shown in Fig. 4.

Only the wave dispersion curves (solid curve in Fig. 4) are presented in Fig. 5. Because the resonance frequency of the AE sensors used in this study was 60 kHz, a single frequency of 60 kHz was chosen for the measurement of the time difference of the group waves. The corresponding time differences at 60 kHz in the dispersion curve of Fig. 5 are listed in Table 1.

Typically, the AE wave velocity should be determined in advance for AE source localization. It is not difficult to measure the AE wave velocity in a laboratory; however, it is not easy to measure the AE wave velocity in an in situ rock mass because there are various uncertainties. These include field condition such as heterogeneity of the rock mass, anisotropy, discontinuity, and boundary reflections. Even

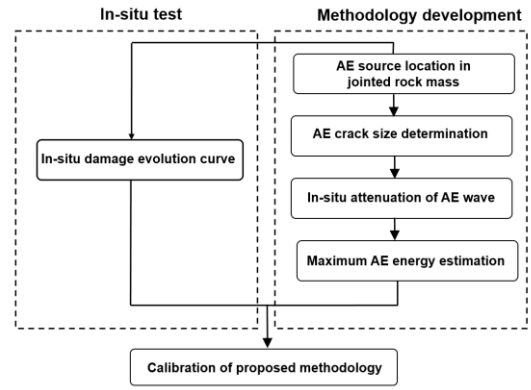


Fig. 3 Flow scheme of this study for a quantitative assessment of in situ rock mass

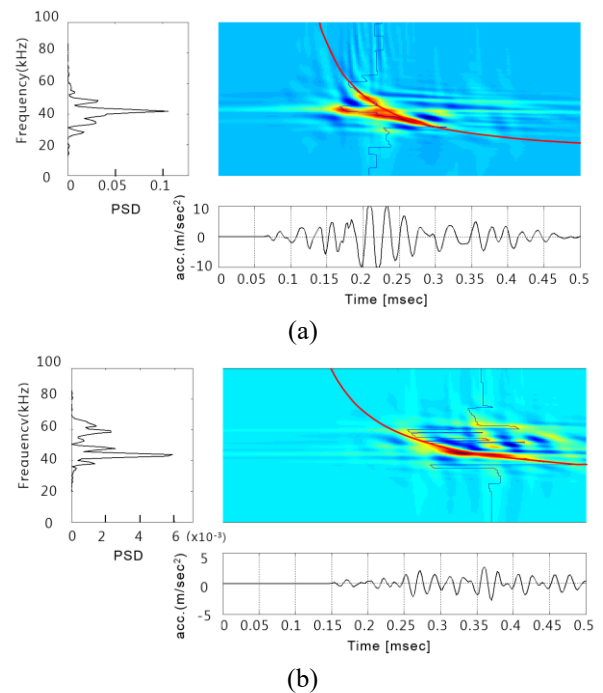


Fig. 4 Time-frequency distribution AE signal and its smoothed WVD (red strongest) superimposed over the theoretical group-velocity curves (red solid line): (a) 4th loading-cycle and (b) 6th loading-cycle

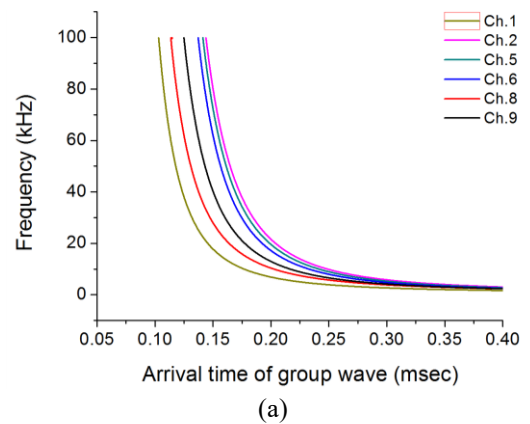


Fig. 5 Theoretical wave dispersion curves: (a) at a time of 115.493 sec in the 4th loading-cycle and (b) at a time of 220.300 sec in the 6th loading-cycle

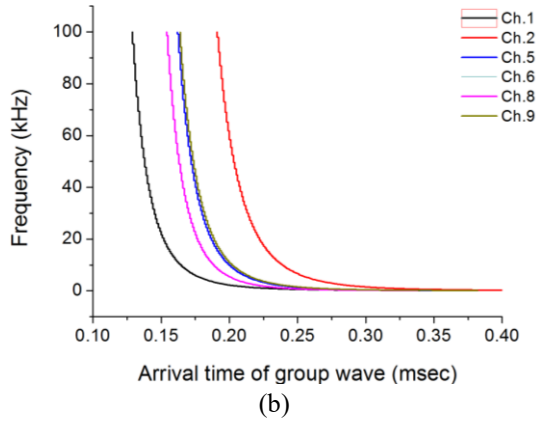


Fig. 5 Continued

Table 1 Arrival time of a group wave at a single frequency of 60 kHz

AE sensor channel	Arrival time of group wave (msec)	
	for 4 <sup>th</sup> cyclic loading	for 6 <sup>th</sup> cyclic loading
Ch.1	0.114	0.135
Ch.2	0.159	0.200
Ch.5	0.156	0.169
Ch.6	0.151	0.171
Ch.8	0.126	0.161
Ch.9	0.138	0.171

if the wave velocity can be measured under such in situ conditions, the value of the wave velocity differs from one position to another. Thus, the concept of ‘minimum variance in velocity’ as proposed by Kim (2013) was used in this study.

The AE source locations coordinates corresponding to the data in Table 1 were determined to be (x, y, z) = (2.8, 50.8, 3.9 cm) for the 4<sup>th</sup> loading-cycle and (-3.2, 44.0, 5.3 cm) for the 6<sup>th</sup> loading-cycle. The average AE source location for a total of 182 AE events was at (-5.1, 38.4, 7.7 cm) and its standard deviation was (9.1, 10.5, 13.4 cm) for the x, y, and z directions, respectively. The 3D AE source locations for the in situ test are presented in Fig. 6, where the center position of the Goodman Jack plate was (0.0, 40.0, 0.0 cm).

3.1.2 Statistical application of the Weibull Distribution

For a quantitative damage assessment in a rock mass, the AE source dimensions should be determined from the in situ test. Gibowicz and Kijko (1994), Brune (1970), and Madariaga (1976) applied a shear model to estimate the fracture source dimensions. However, Cai *et al.* (1998) indicated that a conventional shear model is unrealistically large when comparing the results of an in situ investigation, and suggested the use of a tensile model to estimate the fracture size. This was done by assuming that the tensile fracture is the dominant fracture mechanism for brittle rocks under compressive loading.

However, the tensile model was not easily applicable for this study because the band of effective frequencies of an AE sensor is relatively higher than those of an

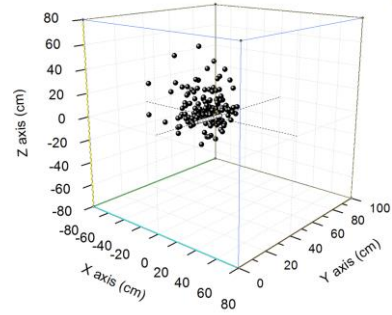
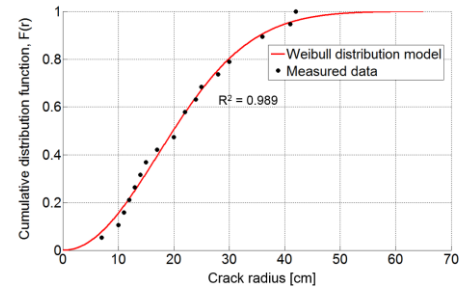
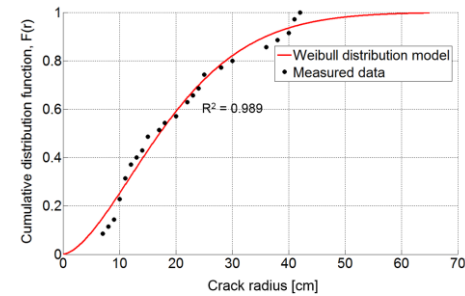


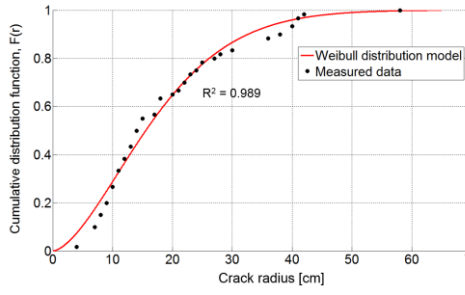
Fig. 6 3D source location of in situ test: an oblique cylinder in the figure represents a loading plate in a borehole



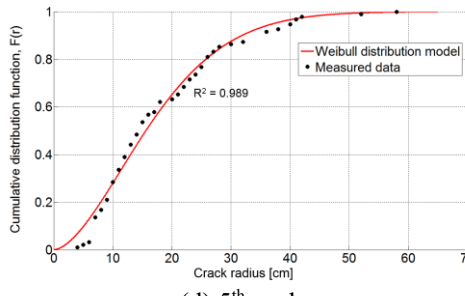
(a) 2<sup>nd</sup> cycle



(b) 3<sup>rd</sup> cycle



(c) 4<sup>th</sup> cycle



(d) 5<sup>th</sup> cycle

Fig. 7 Determination of crack radius corresponding to a 95% probability in a cumulative distribution function for each cycle

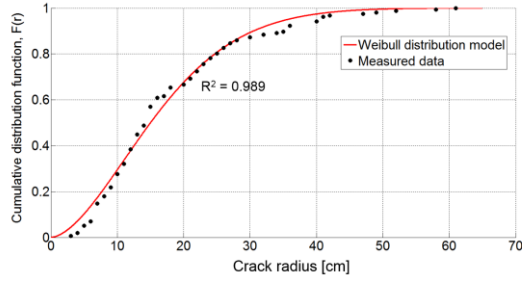
(e) 6<sup>th</sup> cycle

Fig. 7 Continued

accelerometer or a geophone, which are typically used in civil and geotechnical engineering tasks. Moreover an AE wave is very sensitive to heterogeneity, anisotropy, and discontinuity in a rock mass. Thus, one of the statistical approaches, a Weibull function (Weibull 1951), was applied for crack size determination in this study. This function has been widely applied in studies on heterogeneous civil and geotechnical materials such as concrete and rock (Chen and Liu 2004, Dai *et al.* 2012, Fang and Harrison 2002, Atkinson 1987, Tanaka *et al.* 1987).

A Weibull distribution with parameters  $a > 0$  and  $\lambda > 0$  has the following probability density function

$$f(x) = a\lambda^a x^{a-1} e^{-(\lambda x)^a} \quad (3)$$

The cumulative distribution function is

$$F(x) = 1 - e^{-(\lambda x)^a} \quad (4)$$

where  $\lambda$  is the scale parameter of the distribution, and  $a$  is the shape parameter.

All of the AE source location data obtained in Section 3.1.1 were modified to provide the relative distance 'r' with regard to the center of the loading plate of the Goodman Jack, which has a diameter of 76 mm. The relative distance was then fitted using the cumulative distribution function of the Weibull model. The Weibull model was used for each cycle of Goodman Jack loading except for the 1st cycle because very few AE data were detected during the first loading for use in the statistical analysis.

The cumulative distributions of the Weibull model including 2nd, 3rd, 4th, 5th, and 6th cycles are presented in Fig. 7 above. The distance  $r$  corresponding to a 95% probability in a cumulative distribution function was chosen as the crack radius in this study. Cumulative distribution function was derived from the percentile of the probability distribution of crack radius.

The obtained Weibull-distribution function and corresponding crack size for each loading cycle are listed in Table 2. As the number of cycle increases, the crack size increases and converges to a certain value of crack size, and then decreases again.

When the number of cycles was low, the AE location where microcracks were generated became farther from the center of the Goodman Jack plate with increase in the loading stress. As the number of cycles increased and the corresponding loading stress increased, the crack size decreased. This is likely attributable to the fact that more

Table 2 Cumulative Weibull distribution function for each loading cycle of Goodman Jack test

Weibull model		$F(x) = 1 - e^{-(\lambda x)^a}$			
Cycle	Max. stress (MPa)	$\lambda$	$a$	$R^2$	CR* (cm)
2nd	20	0.0421	2.0629	0.992	40.4
3rd	30	0.0465	1.6198	0.979	41.1
4th	40	0.0513	1.6188	0.984	38.4
5th	50	0.0516	1.6816	0.986	37.2
6th	60	0.0537	1.6916	0.989	35.6

\*CR: crack radius of 95% probability in a cumulative distribution function (Fig. 7)

AE cracks are concurrently generated near the peripheral area of the loading plate as the number of cycles and loading stress increase. It was found that the microcracks produced from the Goodman Jack test were centered around the peripheral region of the loading plate of the Goodman Jack, and that the cracks did not surpass a certain size, which is regarded as the critical crack size in this study.

### 3.2 In situ wave attenuation measurement for the correction of AE energy

The frequency characteristics of an observed AE signal depends greatly on the source, media, and propagation distance between the AE source and detector. The source spectrum of an AE is modified during its propagation from the source to the sensor. As the AE wave travels through a geologic material, its amplitude or energy decreases. This effect is known as attenuation and it plays a major role in modifying the AE source spectrum. In general, the attenuation increases with frequency, and thus at large distances from a source, only the low frequency components of AE signals will be detected. Therefore, the in situ attenuation of an AE wave in geological material should be taken into account to determine the AE energy at the crack source location (where the microcracks were generated), rather than at the position of AE sensor (where the AE signals were detected).

The total attenuation is caused primarily by three factors: geometric spreading, material losses (intrinsic attenuation), and apparent attenuation (Winkler *et al.* 1979). This can be expressed as a single equation (Santamarina *et al.* 2001)

$$\frac{A_2}{A_1} = \left( \frac{r_1}{r_2} \right)^\zeta \exp[-\alpha(r_2 - r_1)]T \quad (5)$$

where  $A$  is the wave amplitude, and the exponent of  $\zeta$  is zero in the case of plane waves in infinite media and in rods ( $\zeta=0.5$  for cylindrical fronts, and  $\zeta=1$  for spherical fronts). Variables  $r_1$  and  $r_2$  are the sensing locations,  $\alpha$  is the wave attenuation coefficient, and  $T$  is the transmission coefficient and was assumed to be 1 in this study for simplicity of data analysis.

It is not easy to precisely measure the coefficient  $T$  in situ condition, which is beyond of this research scope.

The reference distance ( $r_1$ ) was fixed to be 1 m. The in

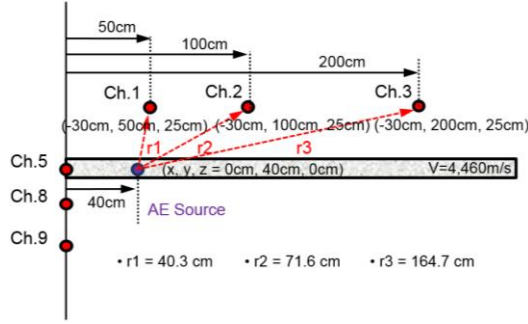


Fig. 8 Sensor locations for the measurement of in situ wave attenuation coefficient (from Fig. 1(b))

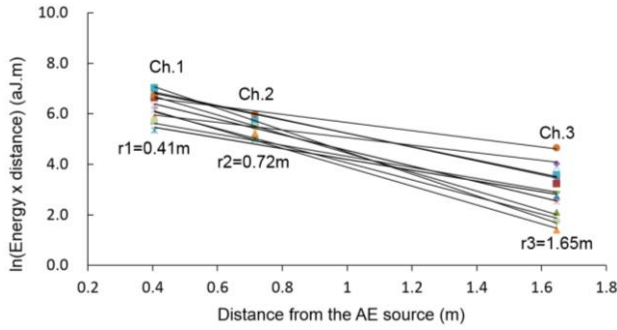


Fig. 9 Measurement of in situ wave attenuation coefficient using AE data at three different locations (Ch. 1, Ch. 2 and Ch. 3)

situ measurements were carried out at three different sensor locations (rather than two) to increase the reliability of the obtained attenuation coefficient. The AE sensors in use were indicated as Ch. 1, Ch. 2 and Ch. 3 in Fig. 8, all of which were the AE sensors drilled and installed in the rock mass.

In this study, an AE energy term was used rather than the wave amplitude of  $A$  in Eq. (5). Carpinteri *et al.* (2007) showed that dissipated energy  $E$  is proportional to the number of AE events, and that AE events are proportional to the amplitude of an AE signal. Qi (2000) suggested that the attenuation of an AE signal is more sensitive than the AE amplitude attenuation. Grosse and Ohtsu (2008) indicated that the energy method is preferred for interpreting the magnitude of an AE source event over AE counts because it is sensitive to the amplitude as well as the duration and is less dependent on the voltage threshold and operating frequencies. Eberhardt *et al.* (1998) also indicated that the AE energy method helps in accentuating AE events with abnormally large amplitudes or durations. Eq. (5) can be expressed in terms of the AE energy as follows:

$$\left(\frac{E_{AE,2}}{E_{AE,1}}\right)^{1/2} = \left(\frac{r_1}{r_2}\right)^{\zeta} \exp[-\alpha'(r_2 - r_1)] \quad (6)$$

The wave attenuation coefficient was estimated using Eq. (6). Only AE signals detected simultaneously at all AE sensors were used in the attenuation investigation. The linear relation among the three locations is presented in Fig. 8.

The in situ wave attenuation equation of the rock mass at the KURT test location can be formulated from Fig. 9 as

$$E(r) = 1726.43 \text{ aJ} \cdot \left(\frac{1}{r}\right) e^{-2.74 r} \quad (7)$$

where  $E(r)$  is the AE energy (aJ, that is,  $10^{-18}$  J) at a distance of  $r$  (m).

### 3.3 Application of fractal theory for scale-independent maximum AE energy

As can be seen in Eq. (1), the maximum AE energy of  $E_{AE,max}$  was determined to derive the degree-of-damage of the KURT rock mass. Thus, it was necessary to infer the maximum AE energy corresponding to the critical crack size determined in Section 3.1.2.

In general, specimens with different sizes and shapes will give different maximum AE energy or AE events at peak strength. Carpinteri and Pugno (2002, 2003) and Carpinteri *et al.* (2004) introduced the fractal fragmentation theory. They suggested that the energy dissipation  $E$ , detected by AE, occurs in a fractal domain composed between a surface and the specimen volume, and subsequently presented a multi-scale criterion to predict the damage evolution. After the fragmentation of rock, the total dissipated energy  $E_{max}$  can be expressed as

$$E_{max} = \Gamma V^{\psi/3} \quad (8)$$

where  $\Gamma$  is the critical value of the fractal energy density,  $V$  is the specimen volume, and  $\psi$  is the fractal exponent, which takes a value between 2 and 3. Turcotte (1992) suggested  $\psi = 1.89$  for artificially crushed quartz,  $\psi = 2.13$  for disaggregated gneiss,  $\psi = 2.22$  for disaggregated granite, and  $\psi = 2.82$  for terrace sand and gravel. In this study,  $\psi = 2.22$  for disaggregated granite was used because the main host rock type of KURT is granite.

In Eq. (8),  $\Gamma$  can be considered a size-independent parameter. Because AE is an elastic wave generated from a rapid release of energy in a material or on its surface, the term of  $E_{max}$  is closely related to the AE energy,  $E_{max,AE}$ . Eq. (8) can be expressed as

$$\log E_{max,AE} = \log \Gamma_{AE} + \frac{\psi}{3} \log V \quad (9)$$

where  $\Gamma_{AE}$  is the critical value of the fractal AE density, not over a volume but over the fractal domain, and can be considered a size-independent parameter. Here,  $E_{max,AE}$  is the maximum AE energy. Consequently, the fractal criterion Eq. (9) predicts a volume-effect on the maximum energy of AE waves and can be expressed as a linear curve with a slope of  $\psi/3$ , which relates  $\log E_{max,AE}$  and  $\log V$  in a logarithmic diagram.

### 3.4 Calibration of quantitative damage with in situ test

Based on the studies described in Section 3.1-3.3, the quantitative degree of damage in the KURT rock mass was inferred and compared with the in situ test results in this section. The maximum AE energy at the peak strength of the KURT rock mass (94.2 MPa) was inferred to be 1,340,371.42 aJ, which was determined using Newton's

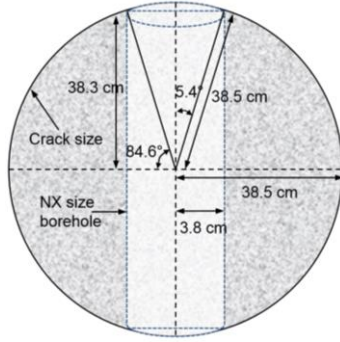


Fig. 10 Crack containing volume in the test borehole (figure not to scale)

iterative method from a previous study (Kim 2013).

Although the estimated maximum crack size during cyclic loading was 41.1 cm (Table 2), the average crack size of 38.5 cm (until the 6th loading-cycle) was used in this study because, in reality, the AEs detected in a rock mass do not show distinct cyclic loading patterns, and it is difficult to distinguish each cyclic stage during in situ AE monitoring. Considering that the distance between Ch.1 and the pseudo-crack source, that is, the periphery of an NX-size (a hole diameter of 76 mm) test borehole was 38.3 cm, the maximum AE energy  $E_{\max,AE}$  at the crack source can be derived from Eq. (7) as follows

$$E_{AE,3.8cm} = E_{AE,38.3cm} \times 3.92 \quad (10)$$

Because the inferred maximum AE energy at 38.3 cm from the periphery of the test borehole was 1,340,3712 aJ at peak strength, the maximum AE energy at the crack source (especially at the surface of the test borehole) was calculated using Eq. (10) to be 5,254,254 aJ.

The volume within which cracks were generated, assumed to be a sphere, was calculated by considering the test borehole geometry. If the volume of the NX-size test borehole was eliminated from the spherical volume (with a crack radius of 38.5 cm), the remaining volume of the rock mass was estimated to be approximately 235,536 cm<sup>3</sup> (Fig. 10).

With regard to the application of fractal theory under the in situ conditions, the calibration factor  $\kappa$  was added to Eq. 9 (as shown in Eq. 11) in this study because the value of  $\Psi$  from the literature was not for an in situ rock mass but for a granite specimen under laboratory conditions. The uncertainty from heterogeneity or discontinuity of a rock mass should be taken into account by considering factor  $\kappa$ .

$$\log E_{\max,AE} = \log \kappa \cdot \Gamma_{AE} + \frac{\Psi}{3} \log V \quad (11)$$

Consequently, Eq. 12 is obtained from Eq. 11 based on values such as the maximum AE energy, crack-size volume, and fractal exponent.

$$\kappa \cdot \Gamma_{AE} = 555.90 \text{ cm}^{-2.22} \quad (12)$$

### 3.4.1 Determination of calibration factor $\kappa$

The in situ data at the 6th cyclic loading was used to

Table 3 Comparison of quantitative degree-of-damage

No. of cycle	Radius of crack size (cm)	AE energy at crack source (aJ): A	Estimated max. AE energy at crack source(aJ): B	Predicted damage (proposed method): A/B	Damage from in situ damage evolution curve
2nd cycle	40.4	28,445	5,850,842	0.01	0.02
3rd cycle	41.1	202,801	6,080,323	0.03	0.04
4th cycle	38.4	436,657	5,221,613	0.08	0.08
5th cycle	37.2	674,495	4,862,738	0.14	0.13

determine the calibration factor  $\kappa$ . The cumulative AE energy at the peak stress of the 6th cycle (i.e., 60 MPa at 2,648 s in Fig. 2(a)) was 312,396 aJ, as shown in Fig. 2. If the in situ attenuation characteristics are taken into account (Eq. 10), the AE energy at the crack source can be estimated as 1,224,592 aJ.

Considering that the crack size in the 6th cycle was 35.6 cm, the subsequent volume containing cracks volume can be calculated as 185,759 cm<sup>3</sup> (in the same manner as in Fig. 10). Consequently, the maximum AE energy at the crack source location was obtained using Eqs. (11) and (12).

$$E_{6th, \max, AE} = 10^{\log \frac{555.90}{\kappa} + \frac{2.22}{3} \log(185,759)} \quad (13)$$

From Fig. 2(b), it was noted that the stress ratio and corresponding degree-of-damage at the 6th loading cycle was 0.64 and 0.23, respectively. A portion of the normalized AE energy at the peak stress of the 6th cycle is, therefore, described as follows

$$\frac{E_{6th}}{E_{6th, \max, AE}} = \frac{1,224,592}{10^{\left(\log \frac{555.90}{\kappa} + \frac{2.22}{3} \log(185,759)\right)}} = 0.23 \quad (14)$$

Consequently, the calculated value of  $\kappa$  was 0.83. The corresponding  $\Gamma_{AE}$  was 669.76 cm<sup>-2.22</sup> from Eq. (12).

### 3.4.2 Comparison of proposed method with in situ test

Based on the obtained values of  $\Gamma_{AE}$  and  $\kappa$ , the quantitative estimation of degree-of-damage at the peak stress of the 4th loading cycle is presented as an example. The crack size in the 4th cycle was 38.4 cm as listed in Table 2 and the AE energy at the peak stress of the 4th cycle was 111,392 aJ (at 1202 s in Fig. 2(a)). If the in situ attenuation characteristics are taken into account (Eq. (10)), the AE energy of the 4th cycle at the crack source ( $E_{4th}$ ) was 436,657 aJ. The crack-size volume was calculated to be 233,698 cm<sup>3</sup>. The corresponding maximum AE energy at the crack size of the 4th cycle ( $E_{4th, \max, AE}$ ) was also estimated to be 5,221,613 aJ from Eq. 11. Thus, the damage at the 4th cycle can be estimated as 0.084 ( $E_{4th}/E_{4th, \max, AE}$ ). From the damage evolution curve of the KURT rock mass, the relative degree-of-damage at the peak stress of the 4th loading cycle (40 MPa) was 0.08 (Fig. 2b). It was found that the inferred damage was close to that measured in the in situ test.

Comparisons of the quantitative degree-of-damage at the peak stresses for the other cycles with in situ test are indicated in Table 3. It is proven that the damage value

proposed in this study agrees quite well with that from the in situ test (damage evolution curve of the KURT rock mass). The methodology suggested in this study can be regarded as a reasonable approach for quantitative damage assessment.

## 4. Discussion

### 4.1 Utilization of the proposed methodology

The utilization of the proposed methodology is identical to the procedure described in Section 3.4. In addition, if the degree-of-damage is determined from in situ AE monitoring, the correspondent degraded strength of a rock mass can be obtained subsequently from the damage evolution curve by multiplying the stress ratio with the inferred rock mass strength. The detailed procedures for quantifying the rock mass damage is presented in Fig. 11 and summarized as follows:

1) Preferentially, the in situ damage evolution curve of a rock mass (that is, the normalized damage versus normalized stress) is obtained by performing an in situ test and AE monitoring.

2) The AE sources are monitored and located using the AE source localization algorithm applicable to the in situ rock mass.

3) The AE crack size is determined by applying the statistical approach of the Weibull distribution model.

4) The in situ wave attenuation for AE energy correction is measured.

5) The AE energy monitored at the position of the AE sensor is corrected to that at the crack source location by taking into account the in situ wave attenuation characteristics

6) The maximum AE energy corresponding to the AE crack size is estimated through the application of fractal theory, and is used as a denominator for the normalized degree of damage.

7) The quantitative degree of damage is estimated by normalizing the AE energy with the maximum AE energy.

8) The stress ratio corresponding to the estimated degree-of-damage in the previously obtained damage evolution curve of the rock mass is determined.

9) The degraded strength of the rock mass is inferred by multiplying the rock mass strength with the stress ratio.

10) The damage evolution of a rock mass is predicted based on the previously determined in situ damage evolution curve.

By continuously upgrading the effects of damage on the effective modulus or strength based on AE monitoring and the in situ damage evolution function, the nonlinear stress-strain response of a rock mass can be more reliably analyzed. Subsequently, it is available to predict the long-term stability of a repository from a numerical study.

### 4.2 Limitations and future works

This study was focused on the introduction of a new approach for quantitative damage assessment of a rock mass. However, more comprehensive studies and a

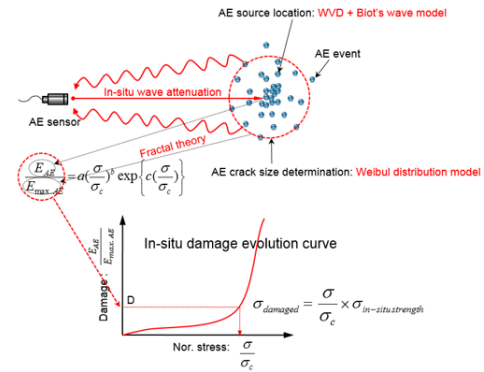


Fig. 11 Utilization of the proposed methodology for a quantitative damage assessment of a rock mass

systematic approach are still required to confirm the validity and reliability of the methodology suggested in this study.

First, the methodology development was based on an in situ test performed under the condition of controlled incremental cyclic loading. Because the failure mechanisms between artificial crack generation by Goodman Jack plate loading and real crack formation under in situ conditions are different, the relation between them and their effects on AE detection should be identified from further research. A micro-seismic wave is sensitive to the degree of saturation, particularly when the soil or rock is saturated with groundwater. Because the AE is composed of relatively high-frequency components, the attenuation of a wave also varies with the degree of saturation. In addition, the effects of groundwater on crack propagation and AE emitting patterns are also of interest. In this study, various assumptions were included, namely, that the crack volume is spherical in shape and its size can be statistically inferred. Thus, the uncertainty associated with such assumptions needs to be identified through a further study.

## 5. Conclusions

This new methodology for quantifying rock mass damage is based on the application of various theoretical approaches in consideration of an AE source-location algorithm applicable to a rock mass, a statistical Weibull model for crack size determination, in situ AE wave attenuation for AE energy correction in the rock mass, and finally, fractal theory for scale-independent AE energy. The developed methodology was calibrated using in situ results from a test that was carried out in the KURT as a part of preceding research. The degree-of-damage at the peak stress of each cycle agrees quite well with that from the in situ test. In addition, once the degree of damage was determined from the in situ AE monitoring using the newly developed methodology, the correspondent degraded strength of a rock mass could be subsequently derived from the damage evolution curve by multiplying the inferred rock mass strength to the stress ratio.

Consequently, provided that the in situ damage evolution curve of a rock mass is obtained in advance from an in situ test, a real-time quantitative damage assessment of a rock mass would be available based on the method

proposed in this study and subsequent AE monitoring. Thus, it is anticipated that the present study could contribute to opening up a way to the quantification of rock mass damage from micro-seismic observations in a waste repository.

## Acknowledgements

This research was supported by the Nuclear Research and Development Program (NRF-2017M2A8A5014857) and the Engineering Research Center (NRF-2017R1A5A1014883) of National Research Foundation of Korea funded by the Korea government (Ministry of Science and ICT).

## References

- ASTM (1981), *Acoustic Emission in Geotechnical Engineering Practice*, American Standard Test Method, Philadelphia, U.S.A.
- Atkinson, B.K. (1987), *Fracture Mechanics of Rock*, University College London, Academic Press, London, U.K.
- Brune, J.N. (1970), "Tectonic stress and the spectra of seismic shear waves from earthquakes", *J. Geophys. Res.*, **75**(26), 4997-5009. <https://doi.org/10.1029/JB075i026p04997>.
- Cai, M., Kaiser, P.K. and Martin, C.D. (1998), "A tensile model for the interpretation of microseismic events near underground openings", *Pure Appl. Geophys.*, **153**, 67-92. [https://doi.org/10.1007/978-3-0348-8804-2\\_5](https://doi.org/10.1007/978-3-0348-8804-2_5).
- Cai, M., Kaiser, P.K. and Martin, C.D. (2001), "Quantification of rock mass damage in underground excavations from microseismic event monitoring", *Int. J. Rock Mech. Min. Sci.*, **38**(8), 1135-1145. [https://doi.org/10.1016/S1365-1609\(01\)00068-5](https://doi.org/10.1016/S1365-1609(01)00068-5).
- Carpinteri, A. and Pugno, N. (2002), "Fractal fragmentation theory for shape effects of quasi-brittle materials in compression", *Mag. Concr. Res.*, **54**(6), 473-480.
- Carpinteri, A. and Pugno, N. (2003), "A multifractal comminution approach for drilling scaling laws", *Powder Technol.*, **131**(1), 93-98. [https://doi.org/10.1016/S0032-5910\(02\)00335-2](https://doi.org/10.1016/S0032-5910(02)00335-2).
- Carpinteri, A., Lacidogna, G. and Pugno, N. (2004), "Scaling of energy dissipation in crushing and fragmentation: A fractal and statistical analysis based on particle size distribution", *Int. J. Fract.*, **129**(2), 131-139. <https://doi.org/10.1023/B:FRAC.0000045713.22994.f2>
- Carpinteri, A., Lacidogna, G. and Pugno, N. (2007), "Structural damage diagnosis and life-time assessment by acoustic emission monitoring", *Eng. Fract. Mech.*, **74**(1-2), 273-289. <https://doi.org/10.1016/j.engfracmech.2006.01.036>.
- Chen, B. and Liu, J. (2004), "Experimental study on AE characteristics of three-point-bending concrete beams", *Cem. Concr. Res.*, **34**(3), 391-397. <https://doi.org/10.1016/j.cemconres.2003.08.021>.
- Dai, Q., Ng, K., Zhou, J., Kreiger, E.L. and Ahlborn, T.M. (2012), "Damage investigation of single-edge notched beam tests with normal strength concrete and ultra high performance concrete specimens using acoustic emission techniques", *Constr. Build. Mater.*, **31**, 231-242. <https://doi.org/10.1016/j.conbuildmat.2011.12.080>.
- Eberhardt, E., Stead, D., Stimpson, B. and Read, R.S. (1998), "Identifying crack initiation and propagation thresholds in brittle rock", *Can. Geotech. J.*, **35**(2), 222-233. <https://doi.org/10.1139/t97-091>.
- EC (2004a), "Geological disposal of radioactive wastes produced by nuclear power: From concept to implementation", EUR21224; European Commission, Belgium.
- EC (2004b), "Thematic network on the role of monitoring in a phased approach to geological disposal of radioactive waste", Final Report to the European Commission Contract FIKW-CT-2001-20130.
- Emsley, S., Olsson, O., Stenberg, L., Alheid, H.J. and Falls, S. (1997), "ZEDEX-a study of damage and disturbance from tunnel excavation by blasting and tunnel boring", Technical Report 97-30, Swedish Nuclear Fuel and Waste Management Co., Sweden.
- Fang, Z. and Harrison, J.P. (2002), "Development of a local degradation approach to the modeling of brittle fracture in heterogeneous rocks", *Int. J. Rock Mech. Min. Sci.*, **39**(4), 443-457. [https://doi.org/10.1016/S1365-1609\(02\)00035-7](https://doi.org/10.1016/S1365-1609(02)00035-7).
- Gibowicz, S.J. and Kijko, A. (1994), *An Introduction to Mining Seismology*, Academic press, New York, U.S.A.
- Grosse, C.U. and Ohtsu, M. (2008), *Acoustic Emission Testing: Basics for Research-Application in Civil Engineering*, Springer, Berlin, Germany.
- Hardy, H.R. (1994), "Geotechnical field applications of AE/MS techniques at the Pennsylvania state university: A historical review", *NDT&E Int.*, **27**(4), 191-200. [https://doi.org/10.1016/0963-8695\(94\)90444-8](https://doi.org/10.1016/0963-8695(94)90444-8).
- IAEA (2001), "Monitoring of geological repositories for high level radioactive waste", IAEA-TECDOC-1208, Austria.
- Jin, P., Wang, E. and Song D. (2017), "Study on correlation of acoustic emission and plastic strain based on coal-rock damage theory", *Geomech. Eng.*, **12**(4), 627-637. <https://doi.org/10.12989/gae.2017.12.4.627>.
- Kim, J.S. (2013), "Quantitative damage assessment of in-situ rock mass using acoustic emission technique", Ph.D. Dissertation, KAIST, Daejeon, Korea.
- Kim, J.S., Lee, K.S., Cho, W.J., Choi, H.J. and Cho, G.C. (2013), "A combined method of Wigner-Ville distribution with a theoretical model for acoustic emission source location in a dispersive media", *KSCE J. Civ. Eng.*, **17**(6), 1284-1292. <https://doi.org/10.1007/s12205-013-0418-6>.
- Kim, J.S., Lee, K.S., Cho, W.J., Choi, H.J. and Cho, G.C. (2014), "A comparative evaluation of stress-strain and acoustic emission methods for quantitative damage assessment of brittle rock", *Rock Mech. Rock Eng.*, **48**(2), 495-508. <https://doi.org/10.1007/s00603-014-0590-0>.
- Ma, K., Tang C.A., Liang, Z.Z., Zhuang, D.Y. and Zhang Q.B. (2017), "Stability analysis and reinforcement evaluation of high-steep rock slope by microseismic monitoring", *Eng. Geol.*, **218**, 22-38. <https://doi.org/10.1016/j.enggeo.2016.12.020>
- Madariaga, R. (1976), "Dynamics of an expanding circular fault", *Bull. Seismol. Soc. Am.*, **66**, 639-666.
- Martin, C.D. and Chandler, N.A. (1994), "The progressive fracture of Lac du Bonnet granite", *Int. J. Rock Mech. Min. Sci. Geomech. Abstr.*, **31**(6), 643-659. [https://doi.org/10.1016/0148-9062\(94\)90005-1](https://doi.org/10.1016/0148-9062(94)90005-1)
- Martin, C.D. and Read, R.S. (1996), "AECL's Mine-by experiment: A test tunnel in brittle rock", *Proceedings of the 2nd North American Rock Mech. Symposium*, Montreal, Canada, June
- Meng, Q., Zhang, M., Han, L., Pu, H. and Chen, Y. (2018), "Acoustic emission characteristics of red sandstone specimens under uniaxial cyclic loading and unloading compression", *Rock Mech. Rock Eng.*, **51**(4), 969-988. <https://doi.org/10.1007/s00603-017-1389-6>.
- Qi, G. (2000), "Attenuation of acoustic emission body waves in acrylic bone cement and synthetic bone using wavelet time-scale analysis", *J. Biomed. Mater. Res.*, **52**(1), 148-156. [https://doi.org/10.1002/1097-4636\(200010\)52:1<148::AID-JBM19>3.0.CO;2-6](https://doi.org/10.1002/1097-4636(200010)52:1<148::AID-JBM19>3.0.CO;2-6).
- Rao, M.V.M.S. and Ramana, Y.V. (1992), "A study of progressive

- failure of rock under cyclic loading by ultrasonic and AE monitoring techniques”, *Rock Mech. Rock Eng.*, **25**(4), 237-251. <https://doi.org/10.1007/BF01041806>.
- Santamarina, J.C., Klein, K.A. and Fam, M.A. (2001), *Soils and Waves*, John Wiley & Sons Ltd., New York, U.S.A.
- Tanaka, T., Nishijima, S. and Ichikawa, M. (1987), *Statistical Research on Fatigue and Fracture*, Elsevier, London, U.K.
- Tang, C., Li, L., Xu, N. and Ma, K. (2015), “Microseismic monitoring and numerical simulation on the stability of high-steep rock slopes in hydropower engineering”, *J. Rock Mech. Geotech. Eng.*, **7**(5), 493-508. <https://doi.org/10.1016/j.jrmge.2015.06.010>.
- Turcotte, D.L. (1992), *Fractals and Chaos in Geology and Geophysics*, Cambridge University Press, Cambridge, U.K.
- Ville, J. (1948), “Théorie et applications de la notion de signal analytique”, *Cables Transmissions*, **2A**(1), 61-74.
- Wang, S.H., Lee, C.I., Ranjith, P.G. and Tang, C.A. (2009), “Modeling the effects of heterogeneity and anisotropy on the excavation damaged/ disturbed zone”, *Rock Mech. Rock Eng.*, **42**(2), 229-258. <https://doi.org/10.1007/s00603-009-0177-3>.
- Weibull, W.A. (1951), “A statistical distribution function of wide applicability”, *J. Appl. Mech.*, **18**(3), 292-297.
- Wigner, E. (1932), “On the quantum correction for thermodynamic equilibrium”, *Phys. Rev.*, **40**, 749-759.
- Winkler, K., Nur, A. and Gladwin, M. (1979), “Friction and seismic attenuation in rocks”, *Nature*, **227**(5697), 528-531. <https://doi.org/10.1038/277528a0>.
- Yang S.Q. and Jing H.W. (2013), “Evaluation on strength and deformation behavior of red sandstone under simple and complex loading paths”, *Eng. Geol.*, **164**, 1-17. <https://doi.org/10.1016/j.enggeo.2013.06.010>.

V

Volume of specimen

 $\psi$ 

Fractal exponent

CC

### List of symbols

$E_{AE}$	Cumulative AE energy
$E_{max.AE}$	Maximum cumulative AE energy at failure
$E_{AE}/E_{max.AE}$	Degree-of-damage, damage parameter D
$\sigma$	Compressive stress
$\sigma_c$	Compressive strength of rock mass
$\lambda$	Scale parameter of Weibull distribution model
$a$	Shape parameter of Weibull distribution model
$r_1, r_2$	Relative distance of wave propagation
$A$	Wave amplitude
$\zeta$	Exponent of wave attenuation
$\alpha$	Wave attenuation coefficient
$T$	Transmission coefficient
$\Gamma$	Critical value of the fractal energy density